Stereoselective ring-opening polymerization of functional β-lactones: influence of the exocyclic side-group

Rama Shakaroun, Hui Li, Philippe Jéhan, Marielle Blot, Ali Alaaeddine,
Jean-François Carpentier, Sophie M. Guillaume

HAL Id: hal-03326803
https://univ-rennes.hal.science/hal-03326803

Submitted on 15 Sep 2021

Stereoselective Ring-Opening Polymerization of Functional β-Lactones: Influence of the Exocyclic Side-Group †

Rama M. Shakaroun,[a,b,‡] Hui Li,[a,‡] Philippe Jéhan,[c] Marielle Blot,[a] Ali Alaaeddine,[b] Jean-François Carpentier,*[a] and Sophie M. Guillaume*[a]

[a] Univ. Rennes, CNRS, Institut des Sciences Chimiques de Rennes, UMR 6226, F-35042 Rennes, France. E-mail: sophie.guillaume@univ-rennes1.fr, jean-francois.carpentier@univ-rennes1.fr

[b] Univ. Libanaise, Campus Universitaire Rafic Hariri Hadath, Faculté des Sciences, Laboratoire de Chimie Médicinale et des Produits Naturels, Beirut, Lebanon.
E-mail: Alikassem.alaaeddine@ul.edu.lb

[c] Centre Régional de Mesures Physiques de l'Ouest-CRMPO, ScanMAT UMS 2001, Université de Rennes 1, France

† Electronic Supplementary Information (ESI) available: kinetics of the polymerizations of BPL^{FG}s, and complementing NMR and MS spectra, TGA, DSC thermograms of the BPL^{FG}s and PBPL^{FG}s. See DOI: 10.1039/x0xx00000x

‡ These authors performed all the experimental work (except the mass spectrometry (P.J.) and chiral HPLC (M.B.) analyses) and contributed to the writing of the paper.

Abstract

Polyhydroxyalkanoates (PHAs) are a unique class of polyesters especially due to their chemical diversity imparted by their side-chain substituent that provides a handle to tune their properties, such as their thermal, mechanical and (bio)degradability signature. Here, we report that some functional PHAs, namely PBPL^{FG}s (FG = functional group), were synthesized by the controlled stereoselective ring-opening polymerization (ROP) of *racemic* 4-substituted-β-propiolactones, namely *rac*-BPL^{CH_2ZPh}s with Z = O, S, CH$_2$OCH$_2$, catalyzed by diamino- or amino-alkoxy-bis(phenolate) yttrium amido complexes (**1a–1g**) in the presence of isopropanol. Unprecedented syndio-enriched (P_r up to 0.87) PBPL^{CH_2ZPh}s of high molar mass ($M_{n,NMR}$ up to 86,400 g mol^{-1}, $Đ_M$ < 1.23) were thus typically prepared under mild operating conditions (toluene, 20 °C). Catalyst systems with smaller "uncrowded" Me or Cl *ortho*-substituents installed on the yttrium phenolate ligands (**1a–1c**) typically revealed less active than those with larger bulkier *t*Bu or CMe$_2$Ph groups (**1d–1g**), regardless of the monomer (TOF$_{1a-1c}$ = 0.48–15 h^{-1}, TOF$_{1d-1g}$ = 450–1840 h^{-1}). Irrespective of the catalyst system, exchanging oxygen with sulphur in BPL^{CH_2ZPh}s, with Z = O, S, did not affect the stereochemistry, always affording syndiotactic PBPL^{CH_2ZPh}s. On the other hand, either atactic or syndiotactic PBPL^{CH_2CH_2OCH_2Ph}s were formed upon tuning the catalyst from **1a–1c** or **1d–1g**, respectively. The intimate relationship, through "non-covalent" interactions, between the chemical nature of the exocyclic functional side-group on the β-lactone and the stereoelectronic tuning arising from the phenolate ligand *ortho*-substituents within the yttrium coordination sphere, modulated the stereocontrol of the ROP. The thermal behavior of these original functional PHAs depended closely on their side-chain substituent (T_d^{onset} = 226 to 272 °C; T_g = −15 to +40 °C).

Keywords: cyclic ester, functional β-propiolactone, β-lactone, non-covalent interactions, polyester, poly(hydroxyalkanoate) (PHA), ring-opening polymerization (ROP), stereoselective catalysis, yttrium

Graphical abstract
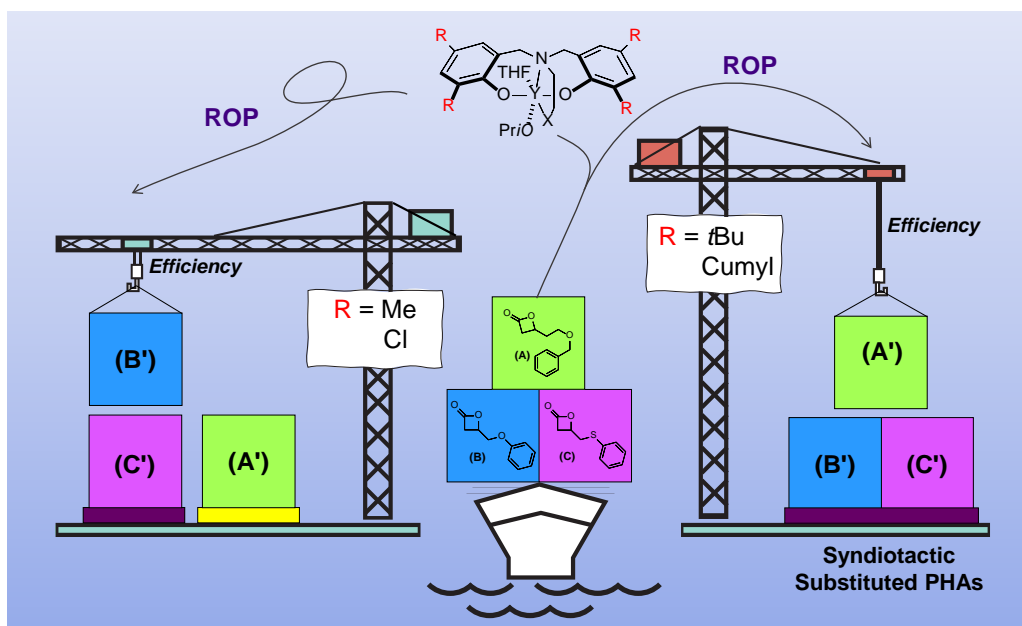
Introduction

Poly(β-hydroxyalkanoate)s (PHAs) are an important family of diversified natural and synthetic aliphatic polyesters renowned for their biodegradation in various environments. While natural PHAs are derived from biorenewable resources and produced by bacteria, synthetic PHAs are formed by ring-opening polymerization (ROP) of β-lactones. PHAs also differ one from another by the side-chain at the β-position of the repeating units along the backbone. Introduction of a pendant functional group (FG) along the polyester chains enables to access to chemically reactive PHAs and to polymers with different and tunable physico-chemical properties, thereby widening their range of applications.[1,2] Within a worldwide increasing market, PHA materials can partially substitute any of the traditional fossil-based polymer families, especially polypropylene (PP) and polyethylene (PE); thus, their uses range from injection molding, extrusion, thermoforming, 3D printing, to foams, non-wovens, fibers, coatings, glues, adhesives, and paints. Besides, owning to their biocompatibility and biodegradability, PHAs are also being used in pharmaceutical, biomedical, cosmetic and packaging applications.[3] PHAs are thus of topical interest especially as versatile green alternatives to single-use plastics with minimal environmental impact.[4]

Natural PHAs are isotactic crystalline polymers, as exemplified with poly(3-hydroxybutyrate) (PHB), the most ubiquitous PHA with a methyl group on the β-carbon, that displays a melting temperature (T_m) of 170–180 °C and a relatively low degradation temperature (ca. 256 °C), thus making difficult its processability and thereby somewhat limiting its commercial applications.[5] Several features have been reported to influence the thermal properties of PHAs. Besides the nature of the side-chain, tacticity is one of the most critical determinants. Isotactic or syndiotactic stereoregular polymers are typically crystalline materials that display improved thermal and mechanical properties relative to their atactic counterparts. Therefore, developing synthetic strategies toward stereoregular PHAs is of great interest.

In this regard, the stereoselective ROP of chiral cyclic esters is a highly topical research field. A challenging objective is the synthesis of functional PHAs with a microstructure different from the naturally occurring isotactic PHAs, namely the

4

ACCEPTED MANUSCRIPT

preparation of syndiotactic PHAs from readily available *racemic* β-lactone monomer(s). Extensive research over the past decades has demonstrated that rare-earth complexes combined with tetradentate bis(phenolate) ligands are highly efficient catalysts/initiators for the controlled ROP of chiral cyclic esters/carbonates, thereby affording synthetic polyesters/polycarbonates with different tacticities.[6,7,8,9,10,11,12] In particular, achiral yttrium complexes with tripodal dianionic diamino- or amino-alkoxy-bis(phenolate) ligands {ONXO}$^{2-}$ (X = NMe$_2$, OMe) are, in the presence of an initiator (typically exogenous isopropanol), regarded as a "privileged" class of catalysts, due to their ability to promote the controlled ROP of heterocyclic monomers, their very high activity, and especially in light of their high stereoselectivity in the ROP of chiral cyclic esters such as of the ubiquitous *racemic* lactide,[12] or of *racemic trans*-cyclohexyl-ring-fused γ-butyrolactone (*rac*-GBL),[13] *racemic trans*-cyclohexene carbonate,[14] and of particular interest to our present research, the more reluctant-to-polymerize four membered-ring *racemic* β-lactones (BPL^{FG})[12,15,16] (Scheme 1). It was thus previously demonstrated that yttrium complexes incorporating bulky aryl-containing substituents at the *ortho* positions of the phenolate ligands enable to access highly syndio-enriched PBPL^{Me} (i.e. PHB) from *racemic* β-butyrolactone (*rac*-BPL^{Me}) with a probability for syndiotactic enchainment (P_r = probability of racemic linkage; P_r = 1 for a perfectly syndiotactic polymer, P_r = 0 for an isotactic one, and P_r = 0.5 for an atactic one) up to 0.94.[12c] These yttrium complexes also successfully promote the stereoselective ROP of higher functional cyclic esters such as the alkyl β-malolactonates (4-alkoxycarbonyl-β-lactones, BPL^{CO_2R} with R = allyl (All = CH$_2$CH=CH$_2$), benzyl (Bn = CH$_2$Ph)).[15] Only the yttrium catalyst bearing small chloro, fluoro or methyl substituents installed at the *ortho* positions on the phenolate rings afford highly syndiotactic PBPL^{CO_2R} (P_r > 0.98), while the incorporation of sterically crowded alky/aryl substituents (typically CMe$_2$*t*-Bu, CMe$_2$Ph = cumyl, CPh$_3$) on the aromatic rings provide significantly less syndio-enriched PBPL^{CO_2R} (P_r = 0.68–0.87). Subsequently, the first highly stereoselective ROP of 4-alkoxymethylene-β-propiolactones (*rac*-BPL^{CH_2OR}s, R = Me, All, Bn) by such yttrium complexes giving PBPL^{CH_2OR}s was reported.[16] It was evidenced that a simple modification of the R *ortho*-

5

substituents on the $\{ONXO^{R2}\}^{2-}$ platform of the yttrium catalyst from dicumyl to dichloro, induced a complete switch from a syndioselective (P_r up to 0.91) to an isoselective (P_m up to 0.93) polymerization of rac-BPL^{CH2OR}s, respectively. DFT computations, focused on the first steps of these ROPs, attributed the origin of the isoselectivity to strong C−H···Cl "second-sphere" or "non-covalent" interactions (NCIs) between the methylene hydrogens in the ring-opened monomer of the growing chain (−CHC*H2*(OC*H2*CH=CH₂)) and the *chloro* substituents of the ligand. Such NCIs arise from the attractive interactions induced by the halogen *ortho*-substituents on the phenolate ligand onto the methylene hydrogens of the last inserted monomer unit within the growing polymer chain.
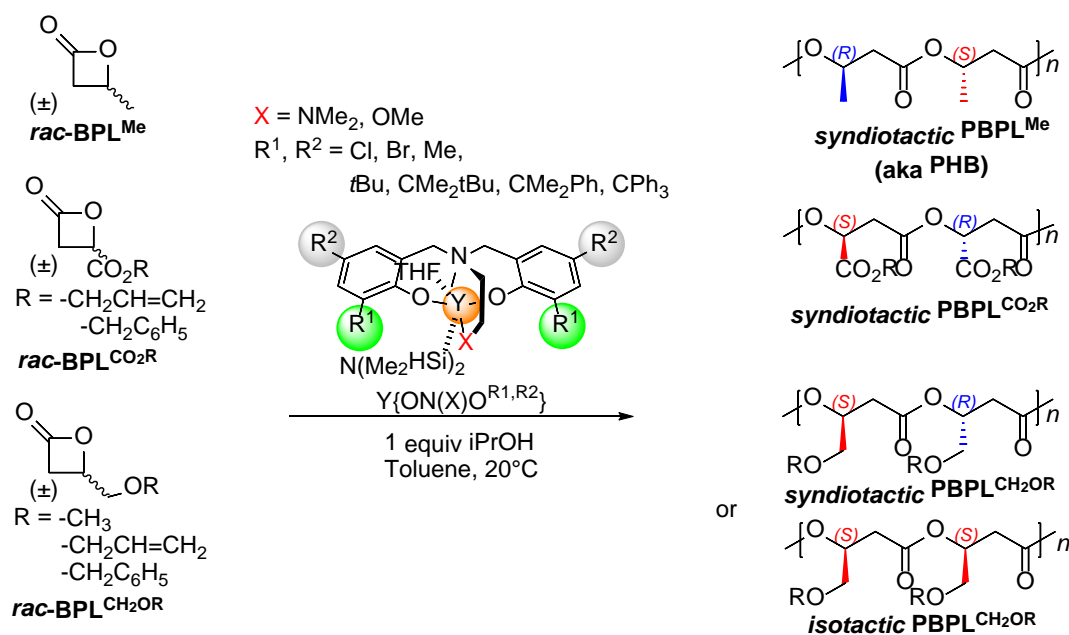
Scheme 1. Stereoselective ROP of various chiral *racemic* 4-substituted-β-propiolactones *rac*-BPL^{FG}s (FG = Me, CO₂R, CH₂OR; R = Me, All, Bn) catalyzed by diamino- or amino-alkoxy-bis(phenolate) yttrium isopropoxide Y$\{ON(X)O^{R1,R2}\}$/*i*PrOH, affording the corresponding PBPL^{FG}s, reported in the litterature.[8,12,15,16]

In this contribution, we first report the synthesis of the unprecedented functional PBPL^{CH2ZPh}s by the ROP of the corresponding newly synthesized *racemic* β-propiolactones BPL^{CH2ZPh}s (except of BPL^{CH2OPh}, *vide infra*)[17], promoted by diamino-

6

ACCEPTED MANUSCRIPT

or amino-alkoxy-bis(phenolate) yttrium catalysts (**1a–1g**) in the presence of *i*PrOH as co-initiator (Scheme 2). These novel PHAs have then been thoroughly characterized by NMR spectroscopy, mass spectrometry, SEC, TGA and DSC analyses. Focus is next placed on the evaluation of the activity and the stereoselectivity of the catalyst systems, in relation to the chemical nature of the exocyclic pendant chain of the β-lactone combined to the stereoelectronic effects imparted by the yttrium ancillary ligand. The effect of the "O" vs "S" heteroatom on the polymerization of the substituted-β-propiolactones BPL^{CH_2ZPh}s (Z = O, S) is assessed. Comparison of the reactivity of *rac*-BPL^{FG}s, where FG = CH_2OPh vs CH_2OR^{16} and $COOR^{15}$ with R = Me, All, Bn, is also reported. Finally, insights into the contribution to the stereoselectivity control of exocyclic methylene hydrogens apart from the central oxygen within the side-arm of 4-alkoxyalkylidene-β-propiolactones, namely *rac*-BPL^{FG}s where FG = C*H₂*OPh or CH₂C*H₂*OC*H₂*Ph vs CH₂OC*H₂*Ph[16], is probed.
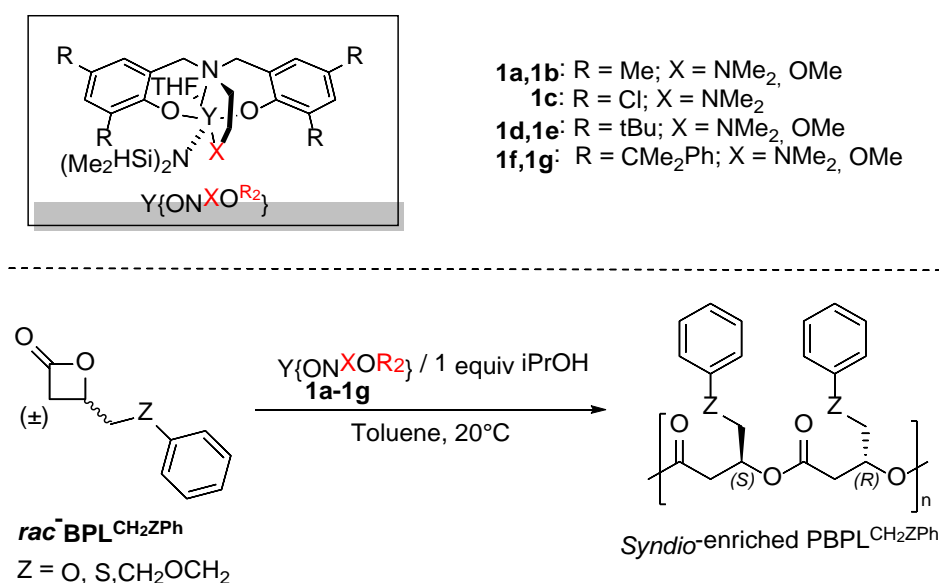
Scheme 2. Stereoselective ROP of chiral 4-substituted-β-propiolactones *rac*-BPL^{CH_2ZPh}s (Z = O, S, CH_2OCH_2) catalyzed by diamino- or amino-alkoxy-bis(phenolate) yttrium complexes $Y\{ONXO^{R_2}\}$ **1a–1g** in the presence of *i*PrOH, investigated in the present work.

7

Experimental section

Methods and materials

All manipulations involving organometallic catalysts were performed under inert atmosphere (argon, < 3 ppm O_2) using standard Schlenk, vacuum line, and glovebox techniques. Solvents were freshly distillated from Na/benzophenone under argon and degassed thoroughly by freeze-thaw-vacuum cycles prior to use. Isopropyl alcohol (Acros) was distilled over Mg turnings under argon atmosphere and kept over activated 3–4 Å molecular sieves. Bisphenol {ONXO^{R_2}}H_2 proligands and yttrium amide precursors of **1a**−**1g** were synthesized according to the methods reported in the literature.[12b, 18] *Racemic* glycidyl phenyl ether (*rac*-G^{CH_2OPh}) was dried onto and distilled from CaH_2 and then stored over 3–4 Å activated molecular sieves (Sigma). *Racemic* 2-((phenylthio)methyl)oxirane (*rac*-G^{CH_2SPh}) [19] and 2-(2-(benzyloxy)ethyl)oxirane (*rac*-G^{CH_2CH_2OCH_2Ph}) [20] were synthesized according to the literature, dried onto and distillated from CaH_2 and then stored over 3–4 Å activated molecular sieves (Figures S1–S5). Enantiopure (*S*)-phenyl glycidyl ether ((*S*)-G^{CH_2OPh}), (*S*)-2-((phenylthio)methyl)oxirane ((*S*)-G^{CH_2SPh}) and (*R*)-2-(2-(benzyloxy)ethyl)oxirane ((*R*)-G^{CH_2CH_2OCH_2Ph}) were prepared by hydrolytic kinetic resolution (HKR) of the corresponding *racemic* compound following the reported procedure (Figures S1–S5).[21] *Rac*-BPL^{CH_2OPh} [17] and [Salph(Cr(THF)$_2$)][Co(CO)$_4$] [22] were synthesized according to the literature procedures. All other reagents were purchased from Aldrich, Sigma or Acros and used as received.

Instrumentation and measurements

^{1}H (500 and 400 MHz) and ^{13}C{^{1}H} (125 and 100 MHz) NMR spectra were recorded on Bruker Avance AM 500 and Ascend 400 spectrometers at 25 °C. ^{1}H and ^{13}C{^{1}H} NMR spectra were referenced internally relative to SiMe$_4$ (δ 0 ppm) using the residual solvent resonances.

Number-average molar mass ($M_{n,SEC}$) and dispersity ($Đ_M = M_w/M_n$) values of the PBPL^{FG}s were determined by size-exclusion chromatography (SEC) in THF at 30 °C (flow rate = 1.0 mL.min^{-1}) on a Polymer Laboratories PL50 apparatus equipped with a refractive index detector and a set of two ResiPore PLgel 3 μm MIXED-D 300 × 7.5

8

mm columns. The polymer samples were dissolved in THF (2 mg.mL^{-1}). All elution curves were calibrated with polystyrene standards; $M_{n,SEC}$ values of the PBPL^{FG}s were uncorrected for the possible difference in hydrodynamic radius *vs.* that of polystyrene.

The molar mass of PBPL^{FG} samples was also determined by ^{1}H NMR analysis in CDCl$_3$ from the relative intensities of the signals of the PBPL^{CH_2ZPh} repeating unit methine hydrogen (δ (ppm): 5.48 –OC*H*(CH$_2$OPh)CH$_2$, PBPL^{CH_2OPh}; 5.26 – OC*H*(CH$_2$SPh)CH$_2$, PBPL^{CH_2SPh}; 5.34 –OC*H*(CH$_2$CH$_2$OCH$_2$Ph)CH$_2$, PBPL^{CH_2CH_2OCH_2Ph}), and of the isopropyl chain-end (δ (ppm): 4.94–4.99 (CH$_3$)$_2$C*H*O–, 1.17–1.20 (C*H$_3$*)$_2$CHO–).

Monomer conversions were calculated from ^{1}H NMR spectra of the crude polymer samples in CDCl$_3$ by using the integration (Int.) ratios Int.$_{PBPL(CH_2OPh)/PBPL(CH_2CH_2OCH_2Ph)}$ / [Int.$_{PBPL(CH_2OPh)/PBPL(CH_2CH_2OCH_2Ph)}$ + Int.$_{BPL(CH_2OPh)/BPL(CH_2CH_2OCH_2Ph)}$], and [Int.$_{PBPL(CH_2SPh)}$ + Int.$_{(2)}$ + Int.$_{(3)}$] / [Int.$_{PBPL(CH_2SPh)}$ + Int.$_{BPL(CH_2SPh)}$ + Int.$_{(2)}$ + Int.$_{(3)}$] (compounds **2** and **3** correspond to the decomposed and rearrangement products of *rac-*BPL^{CH_2SPh}, respectively; *vide infra*) of the methine hydrogens of BPL^{CH_2ZPh} and PBPL^{CH_2ZPh} (corresponding methine hydrogen signal of the polymers (see above), and of the monomers: δ (ppm) 4.85 BPL^{CH_2OPh}, 4.62 BPL^{CH_2SPh}, and 4.71 BPL^{CH_2CH_2OCH_2Ph}).

Mass spectra were recorded at CRMPO-ScanMAT (Rennes, France). ESI mass spectra were recorded on an orbitrap type Thermofisher Scientific Q-Exactive instrument with an ESI source in positive mode by direct introduction with a flow rate of 5–10 µL min^{-1}. Samples were prepared in CH$_2$Cl$_2$ at 10 µg mL^{-1}. High resolution Matrix Assisted Laser Desorption Ionization - Time of Flight, MALDI-ToF, mass spectra were recorded using an ULTRAFLEX III TOF/TOF spectrometer (Bruker Daltonik Gmbh, Bremen, Germany) in positive ionization mode. Spectra were recorded using reflectron mode and an accelerating voltage of 25 kV. A mixture of a freshly prepared solution of the polymer in THF or CH$_2$Cl$_2$ (HPLC grade, 10 mg mL^{-1}) and DCTB (*trans*-2-(3-(4-*tert*-butylphenyl)-2methyl-2-propenylidene) malononitrile, and a MeOH solution of the cationizing agent (NaI, 10 mg mL^{-1}) were prepared. The solutions were combined in a 1:1:1 *v/v/v* ratio of matrix-to-sample-to-cationizing agent.

The resulting solution (0.25–0.5 µL) was deposited onto the sample target (Prespotted AnchorChip PAC II 384 / 96 HCCA) and air or vacuum dried.

Chiral HPLC analysis of (*S*) or (*R*)-G^{FG}s was performed on a Thermofisher Scientific chromatograph equipped with a Chiralcel-OD DAICEL column (250 mm × 4.6 mm, 5 µm) and a UV detector at 214 nm at 20 °C, using for (*S*)-G^{CH_2OPh}: hexane/isopropanol 90:10 *v/v* (1 mL.min^{-1}, 22 bar), (*S*)-G^{CH_2SPh}: hexane/isopropanol 99.5:0.5 *v/v* (0.9 mL.min^{-1}, 23 bar), and (*R*)-$G^{CH_2CH_2OCH_2Ph}$ (0.9 mL.min^{-1}, 23 bar).

Thermal gravimetry analyses (TGA) were performed on a Metler Toledo TGA/DSC1 by heating the polymer samples at a rate of 10 °C min^{-1} from +25 to +600 °C in a dynamic nitrogen atmosphere (flow rate = 50 mL min^{-1}).

Differential scanning calorimetry (DSC) analyses were performed with a Setaram DSC 131 apparatus calibrated with indium, at a rate of 10 °Cmin^{-1}, under a continuous flow of helium (25 mL.min^{-1}), using aluminum capsules. The thermograms were recorded according to the following cycles: −80 to 200 °C at 10 °C min^{-1}; 200 to −80 °C at 10 °C min^{-1}; −80 °C for 5 min; −80 to 200 °C at 10 °C min^{-1}; 200 to −80 °C at 10 °C min^{-1}.

Procedure for the carbonylation of the epoxides into the corresponding β-lactones[17]

Carbonylation of phenyl glycidyl ether (rac-G^{CH_2OPh}) into racemic 4-phenyloxymethylene-β-propiolactone (rac-BPL^{CH_2OPh}). In a typical experiment, in the glovebox, a Schlenk flask was charged with [Salph(Cr(THF)$_2$)][Co(CO)$_4$] (235 mg, 0.26 mmol). On a vacuum line, dry DME (15 mL) was syringed in and the resulting solution was cannulated into a degassed high-pressure reactor, which was pressurized with carbon monoxide to 20 bars, and stirred for 15 min before depressurization. A solution of *racemic*-phenyl glycidyl ether (*rac*-2-(phenyloxymethyl)oxirane) (*rac*-G^{CH_2OPh}) (3.88 g, 25.9 mmol, 100 equiv.) in dry DME (15 mL) was transferred into the reactor, which was then pressurized with CO to 40 bars. The reaction mixture was stirred for 2 days at 20 °C. The reactor was then vented to atmospheric pressure, volatiles were removed under vacuum and the crude product was purified through a silica column (CH$_2$Cl$_2$, 2 × 300 mL). Evaporation of volatiles afforded *rac*-BPL^{CH_2OPh}

10

ACCEPTED MANUSCRIPT

as a white solid that was crystallized from diethyl ether to give pure 4-phenoxymethylene-β-propiolactone (*rac*-BPL^{CH_2OPh}) (3.5 g; 75% yield). ^{1}H NMR (500 MHz, CDCl$_3$, 25 °C) δ (ppm): δ 7.34–7.28 (m, 2H$_g$), 7.03–6.98 (m, 1H$_h$), 6.95–6.91 (m, 2H$_f$), 4.88–4.81 (m, 1H$_c$), 4.33 (dd, *J* = 11, 3 Hz, 1H$_e$), 4.23 (dd, *J* = 11, 4 Hz, 1H$_d$), 3.62–3.53 (m, 2H$_{ab}$) (Figure S6-top). ^{13}C NMR (125 MHz, CDCl$_3$, 25 °C) δ (ppm): 167.3 (*C$_1$*=O), 158.1 (*ipso-C$_5$*), 129.8 (*m-C$_7$*H), 121.9 (*p-C$_8$*H), 114.8 (*o-C$_6$*H), 68.4 (*C$_3$*HOC(O)), 67.4 (*C$_4$*H$_2$OPh), 40.2 (*C$_2$*H$_2$C(O)O) (Figure S6-bottom).

The carbonylation of (*S*)-phenyl glycidyl ether was performed similarly and gave (*S*)-BPL^{CH_2OPh} as an off-white solid (3.45 g, 74% yield) that displayed NMR spectra identical to those of *rac*-BPL^{CH_2OPh}.[17] Both *rac*-BPL^{CH_2OPh} and (*S*)-BPL^{CH_2OPh} were stored under argon in the fridge at −27 °C.

Carbonylation of racemic 2-((phenylthio)methyl)oxirane (rac-G^{CH_2SPh}) to racemic 4-(phenylthio)methylene-β-propiolactone (rac-BPL^{CH_2SPh}). Following the aforementioned typical carbonylation procedure, starting from [Salph(Cr(THF)$_2$)][Co(CO)$_4$] (218 mg, 0.24 mmol) and 2-((phenylthio)methyl)oxirane (*rac*-G^{CH_2SPh}) (4.0 g, 24 mmol, 100 equiv), *racemic* 4-(phenylthio)methylene-β-propiolactone (*rac*-BPL^{CH_2SPh}) was, following purification through a silica column using CHCl$_3$ as eluent followed by drying over 3–4 Å molecular sieves (thus avoiding distillation due to BPL^{CH_2SPh} instability), isolated as a pale yellow viscous liquid (2.4 g, 51% yield). ^{1}H NMR (400 MHz, CDCl$_3$, 25 °C) δ (ppm): δ 7.45–7.40 (m, 2H$_f$), 7.36–7.24 (m, 3H$_{g,h}$), 4.63–4.55 (m, 1H$_c$), 3.50 (dd, *J* = 17, 6 Hz, 1H$_d$), 3.43 (dd, *J* = 14, 5 Hz, 1H$_e$), 3.17–3.11 (m, 2H$_{ab}$) (Figure S7-top). ^{13}C NMR (101 MHz, CDCl$_3$, 25 °C) δ (ppm): 167.3 (*C$_1$*=O), 133.9 (*ipso-C$_5$*), 131.2 (*o-C$_6$*H), 129.4 (*m-C$_7$*H), 127.7 (*p-C$_8$*H), 68.9 (*C$_3$*HOC(O)), 43.0 (*C$_4$*H$_2$SPh), 38.0 (*C$_2$*H$_2$C(O)O) (Figure S7-bottom). ESI-MS *m/z* observed = 217.0293 vs *m/z* calculated = 217.0299 (Figure S8).

The carbonylation of (*S*)-G^{CH_2SPh} was performed similarly and gave (*S*)-BPL^{CH_2SPh} as a pale yellow viscous liquid (2.2 g, 47% yield) that displayed NMR spectra identical to those of *rac*-BPL^{CH_2SPh}. To prevent the degradation of *rac*-BPL^{CH_2SPh} and (*S*)-BPL^{CH_2SPh} (Figure S9),[17] they were both freshly prepared prior to use.

Carbonylation of racemic 2-(2-(benzyloxy)ethyl)oxirane rac-G^{CH_2CH_2OCH_2Ph} to

racemic 4-(2-(benzyloxy)ethylene)-β-propiolactone (rac-BPL^{CH_2CH_2OCH_2Ph}).
Following the aforementioned typical carbonylation procedure, starting from [Salph(Cr(THF)$_2$)][Co(CO)$_4$] (540 mg, 0.50 mmol) and *racemic* 2-(2-(benzyloxy)ethyl)oxirane (*rac*-G^{CH_2CH_2OCH_2Ph}) (8.9 g, 50 mmol, 100 equiv.), *racemic* 4-(2-(benzyloxy)ethylene)-β-propiolactone (*rac*-BPL^{CH_2CH_2OCH_2Ph}) was obtained as a colorless liquid (5.3 g, 52% yield) after evaporation of volatiles and purification through an alumina column using CHCl$_3$ as eluent. ^{1}H NMR (500 MHz, CDCl$_3$, 25 °C) δ (ppm): 2.11 (m, 2H$_d$), 3.20 (dd, J = 16, 4 Hz, 1H$_b$), 3.53 (dd, J = 16, 6 Hz, 1H$_a$), 3.62 (td, J = 5, 2 Hz, 2H$_e$), 4.51 (s, 2H$_f$), 4.71 (m, 1H$_c$), 7.28-7.37 (m, 5H$_g$) (Figure S10-top); ^{13}C NMR (125 MHz, CDCl$_3$, 25 °C) δ (ppm): 168.3 (C_1=O), 138.1 (*ipso*-C_7), 128.5(*o*-C_8H), 127.8 (*o*-C_9H), 127.6 (*o*-C_{10}H), 73.2 (OC_6H$_2$Ph), 69.2 (C_3HCH$_2$CH$_2$O), 65.8(CHCH$_2$$C_5H_2$O), 43.2 ($C_2H_2$C(O)O), 34.7 (CH$C_4H_2CH_2$O) (Figure S10-bottom). ESI-MS *m/z* observed=229.0836 vs *m/z* calculated = 229.0835 (Figure S11).

The carbonylation of (*R*)-G^{CH_2CH_2OCH_2Ph} was performed similarly and gave (*R*)-BPL^{CH_2CH_2OCH_2Ph} as a colorless liquid (1.5 g, 55% yield) that displayed NMR spectra identical to those of *rac*-BPL^{CH_2CH_2OCH_2Ph}. Both *rac*-BPL^{CH_2H_2OCH_2Ph} and (*R*)-BPL^{CH_2CH_2OCH_2Ph} were stored under argon in fridge at −27 °C.

Typical polymerization procedure. In a typical experiment (Table 1, entry 6), in the glovebox, a Schlenk flask was charged with [Y(N(SiHMe$_2$)$_2$)$_3$](THF)$_2$ (8.8 mg, 14 µmol) and {ONNO^{tBu2}}(**1d**, 7.4 mg, 14 µmol), and toluene (0.25 mL) was next added. To this solution, *i*PrOH (107 µL of a 1% (*v/v*) solution in toluene, 1 equiv *vs.* Y) was added under stirring at room temperature (ca. 20 °C). After 5 min of stirring, a solution of *rac*-BPL^{CH_2OPh} (150 mg, 0.84 mmol, 60 equiv) in toluene (0.5 mL) was added rapidly and the mixture was stirred at 20 °C for 1 h. The reaction was quenched by addition of acetic acid (*ca.* 0.5 mL of a 1.6 mol·L^{-1} solution in toluene). The resulting mixture was concentrated to dryness under vacuum and the conversion was determined by ^{1}H NMR analysis of the residue in CDCl$_3$. The crude polymer was then dissolved in CH$_2$Cl$_2$ (*ca.* 1 mL) and precipitated in cold pentane (*ca.* 5 mL), filtered and dried. The PBPL^{CH_2OPh}, PBPL^{CH_2SPh} and PBPL^{CH_2CH_2OCH_2Ph} were recovered as white solid, yellow oil, and colorless oil, respectively. All recovered polymers were then analyzed by NMR spectroscopy,

12

mass spectrometry, SEC, TGA and DSC analyses (Table 1, Figures 1–5,S12–S25).

Results and discussion

The functional 4-substituted-β-propiolactones rac-BPL^{CH_2ZPh}s and the enantiopure (S)-or (R)-BPL^{CH_2ZPh}s (Z = O, S, CH$_2$OCH$_2$) were first prepared in good yields (47−75%) on a multi-gram scale (1.5−5.3 g) from the carbonylation reaction of the corresponding epoxide rac-, (S)- or (R)-G^{CH_2ZPh}s, respectively, according to a typical procedure,[17] and next characterized by NMR spectroscopy and mass spectrometry (MS) analyses (Figures S1−S11). While the synthesis of BPL^{CH_2OPh} was already reported,[17] to our knowledge, its ring-opening homopolymerization has never been described. Only the random copolymerization of BPL^{CH_2OPh} with of BPL^{Me} via anionic simultaneous ring-opening copolymerization using the metal-free tetrabutylammonium acetate initiator was established to next study the resulting oligomers ($M_{n,SEC}$ = 1200 g mol^{-1}) by mass spectrometry.[23] In addition, for the first time to our knowledge, a functional β-lactone and PHA featuring a sulphur heteroatom within the exocyclic side-arm, namely BPL^{CH_2SPh} and PBPL^{CH_2SPh}, were prepared herein. Subsequently, the ROP of these original four-membered ring β-lactones was investigated, at room temperature in toluene, using the diamino- or amino-alkoxy-bis(phenolate) yttrium catalytic systems Y{ONXO^{R_2}}/(iPrOH) (**1a−1g**/(iPrOH)), the latter ones differing in terms of the phenolate *ortho*-substituents on the ancillary ligand (Scheme 2). Note that the influence of the *para*-substituents on the phenolate ligand of complexes **1** having been previously shown not to significantly contribute to the performance (especially the activity and the stereoselectivity) of the yttrium catalysts/initiators, they were not considered further in the present studies.[12,15,16] These active catalysts were conveniently generated *in situ* upon addition of 1 equiv. of an exogeneous iPrOH, added as co-initiator to the mixture of the proligand and the yttrium amido precursor [Y(N(SiHMe$_2$)$_2$)$_3$](THF)$_2$, respectively (Scheme 2).[15,16] The kinetics of the NMR-scale ROP of rac-BPL^{CH_2ZPh}s was monitored by ^{1}H NMR spectroscopy. The most significant data for the thus synthesized PBPL^{CH_2ZPh}s are gathered in Tables 1 and S1. The macromolecular characteristics, and especially the microstructure of the recovered PBPL^{CH_2ZPh}s

polyesters, were thoroughly assessed by ^{1}H, ^{13}C{^{1}H} and 2D (COSY, HMBC) NMR spectroscopy (Tables 1,S1; Figures S12–S18), MALDI-ToF MS (Figures S19–S21), SEC (Tables 1,S1), TGA and DSC (Table 1; Figures S22–S25) analyses.

Table 1. Characteristics of the PBPL^{CH_2ZPh}s synthesized by ROP of *rac*-BPL^{CH_2ZPh}s with Z = O, S, CH$_2$OCH$_2$ mediated by **1a−1g**/(*i*PrOH) catalytic systems in toluene at room temperature.

Entry	BPL^{CH_2ZPh}	Cat.	[BPL^{CH_2ZPh}]$_0$/ [1]$_0$/[iPrOH]$_0$ [a]	Time [b] (min)	Conv. [c] (%)	$M_{n,theo}$ [d] (g.mol^{-1})	$M_{n,NMR}$ [e] (g.mol^{-1})	$M_{n,SEC}$ [f] (g.mol^{-1})	$Đ_M$ [f]	P_r [g]	T_g [h] (°C)
1	CH$_2$OPh	**1a**	30:1:1	120	100	5400	5200	6200	1.18	0.76	*nd* [j]
2 [i]	CH$_2$OPh	**1a**	60:1:1	240	95	10 200	10 000	11 100	1.13	0.79	30
3	CH$_2$OPh	**1c**	30:1:1	30 h	95	5100	5000	5200	1.14	0.77	22
4 [i]	CH$_2$OPh	**1c**	60:1:1	50 h	54	5800	5400	6200	1.15	0.75	21
5	CH$_2$OPh	**1d**	20:1:1	120	100	3600	3200	4100	1.21	0.84	*nd* [j]
6 [i]	CH$_2$OPh	**1d**	60:1:1	8	100	10 700	10 600	12 200	1.14	0.86	37
7	CH$_2$OPh	**1d**	120:1:1	8	98	21 000	23 000	25 600	1.06	0.86	37
8	CH$_2$OPh	**1d**	250:1:1	15	100	44 600	44 100	51 200	1.16	0.87	38
9	CH$_2$OPh	**1d**	500:1:1	15	92	81 900	80 500	95 000	1.20	0.86	40
10	CH$_2$OPh	**1f**	28:1:1	120	100	5000	4700	5400	1.20	0.81	*nd* [j]
11 [i]	CH$_2$OPh	**1f**	60:1:1	30	100	10 700	10 000	12 200	1.15	0.84	38
12	CH$_2$OPh	**1f**	100:1:1	8	100	17 900	17 800	19 000	1.11	0.83	40
13	(*S*)-CH$_2$OPh	**1d**	60:1:1	60	100	10 700	10 500	11 700	1.10	<0.05	36
14	CH$_2$SPh	**1a**	30:1:1	240	100	5900	5800	6600	1.14	0.74	9
15 [i]	CH$_2$SPh	**1a**	60:1:1	480	99	11 600	11 300	13 900	1.21	0.76	8
16	CH$_2$SPh	**1c**	20:1:1	240	38	1500	1 400	1700	1.08	*nd* [j]	*nd* [j]
17	CH$_2$SPh	**1c**	30:1:1	60 h	57	3400	3400	3600	1.14	0.73	9
18 [i]	CH$_2$SPh	**1c**	60:1:1	96 h	48	5600	5100	6400	1.17	0.74	9
19	CH$_2$SPh	**1d**	40:1:1	240	100	7800	7400	8900	1.19	0.83	*nd* [j]
20 [i]	CH$_2$SPh	**1d**	80:1:1	60	100	15 600	15 200	17 900	1.15	0.87	13
21	CH$_2$SPh	**1d**	120:1:1	15	100	23 200	23 300	25 700	1.07	0.86	14
22	CH$_2$SPh	**1d**	250:1:1	60	95	46 100	48 300	51 400	1.15	0.87	14
23	CH$_2$SPh	**1d**	500:1:1	120	90	87 400	86 400	96 700	1.17	0.86	12
24	CH$_2$SPh	**1f**	20:1:1	60	100	3900	3400	4400	1.19	0.85	*nd* [j]
25 [i]	CH$_2$SPh	**1f**	60:1:1	60	100	11 700	11 300	13 300	1.12	0.85	13
26	CH$_2$SPh	**1f**	120:1:1	15	95	22 200	23 200	24 600	1.14	0.84	12

27	(S)-CH$_2$SPh	**1d**	60:1:1	60	100	11 700	11 500	12 800	1.13	<0.05	13
28	CH$_2$CH$_2$OCH$_2$Ph	**1a**	50:1:1	9 h	67	7000	8600	7000	1.23	0.49	−12
29	CH$_2$CH$_2$OCH$_2$Ph	**1b**	25:1:1	7.5 h	99	5200	5400	4300	1.48	0.49	*nd*[j]
30	CH$_2$CH$_2$OCH$_2$Ph	**1b**	50:1:1	9 h	87	9000	9550	8000	1.06	0.52	*nd*[j]
31	CH$_2$CH$_2$OCH$_2$Ph	**1c**	25:1:1	14 h	78	4100	5200	4200	1.15	0.49	−15
32	CH$_2$CH$_2$OCH$_2$Ph	**1d**	25:1:1	5	99	5200	6400	6700	1.12	0.85	−11
33	CH$_2$CH$_2$OCH$_2$Ph	**1e**	25:1:1	5	99	5200	5100	6800	1.21	0.80	−13
34	CH$_2$CH$_2$OCH$_2$Ph	**1f**	25:1:1	3	99	5200	5400	4400	1.09	0.77	−12
35	CH$_2$CH$_2$OCH$_2$Ph	**1f**	100:1:1	10	98	20 200	-	19 200	1.05	0.77	*nd*[j]
36	CH$_2$CH$_2$OCH$_2$Ph	**1g**	25:1:1	3	99	5200	6600	5400	1.19	0.86	−13
37	CH$_2$CH$_2$OCH$_2$Ph	**1g**	50:1:1	3	99	10 300	-	8500	1.12	0.81	*nd*[j]
38	CH$_2$CH$_2$OCH$_2$Ph	**1g**	100:1:1	6	99	20 500	-	20 600	1.07	0.85	−9
39	CH$_2$CH$_2$OCH$_2$Ph	**1g**	150:1:1	15	99	31000	-	29800	1.08	0.82	*nd*[j]
40	(R)-CH$_2$CH$_2$OCH$_2$Ph	**1d**	50:1:1	10	99	10 300	9100	8400	1.15	<0.05	−14

[a] Reactions performed with $[BPL^{CH_2ZPh}]_0 = 1.0$ M. [b] Reaction time was not necessarily optimized. [c] Conversion of BPL^{CH_2ZPh} as determined by ^{1}H NMR analysis of the crude reaction mixture. [d] Molar mass calculated according to $M_{n,theo} = ([BPL^{CH_2ZPh}]_0/[1]_0 \times conv._{BPL(CH_2ZPh)} \times M_{BPL(CH_2ZPh)}) + M_{iPrOH}$, with $M_{BPL(CH_2OPh)} = 178$ g.mol^{-1}, $M_{BPL(CH_2SPh)} = 194$ g.mol^{-1}, $M_{BPL(CH_2CH_2OCH_2Ph)} = 206$ g.mol^{-1}, $M_{iPrOH} = 60$ g.mol^{-1}. [e] Molar mass determined by ^{1}H NMR analysis of the isolated polymer, from the resonances of the terminal O*i*Pr group (refer to Experimental section). [f] Number-average molar mass and dispersity (M_w/M_n) determined by SEC analysis in THF at 30 °C *vs.* polystyrene standards. [g] P_r is the probability of *racemic* linkages between BPL^{CH_2ZPh} units as determined by $^{13}C\{^1H\}$ NMR analysis of the isolated PBPL^{CH_2ZPh}s. [h] Glass transition temperature as determined by DSC. [i] Refer to the kinetic study (Table S1); [j] Not determined.

ROP of *rac*-BPL^{CH_2ZPh}s (Z = O, S, CH$_2$OCH$_2$) promoted by 1a–1g/(*i*PrOH) catalyst systems: insights into the catalyst activity and the kinetics

Yttrium catalyst systems based on ligands with small Me or Cl *ortho*-phenolate substituents (**1a–1c**), in the presence of *i*PrOH, proved poorly active regardless of the *rac*-BPL^{CH_2ZPh}, presumably due to the aggregated/dimeric nature of these metal complexes (Table 1, entries 1–4,14–18,28–31).[8b] The Me-substituted catalyst systems **1a,1b**/(*i*PrOH) could achieve near complete conversion of ca. 30 monomer equiv. in a few hours (99−100% yield, i.e. 25−30 equiv. in 2−7.5 h), unlike the Cl-substituted one **1c** which hardly proceeded to complete monomer consumption (57−95% yield, i.e. 17−28 equiv. in 14−60 h) (Table 1, entries 1,14,29;3,17,31). Correspondingly, the best activity achieved by the catalysts as expressed by turnover frequency (TOF) values remained sluggish: TOF$_{1a-b}$ = 4.8−15 h^{-1} vs TOF$_{1c}$ = 1.0−1.4 h^{-1} (Table 1, entries

15

2,15,30;3,16,30). This poor activity of uncrowded alkyl or halogenated catalysts **1a–1c**/(*i*PrOH) contrasted with the moderate-to-high activity recorded in the alike ROP of $BPL^{CH_2OAll/Bn}$ (TOF = 20–30 h^{-1}) or BPL^{CO_2R} (TOF = 1400 h^{-1}) under the same operating conditions.[8b,15,16] On the other hand, yttrium catalyst systems with ancillary ligands bearing bulky substituents (*t*Bu, cumyl, **1d–1g**/(*i*PrOH)) revealed quite active for the ROP of *rac*-BPL^{CH_2ZPh}s, with the cumyl substituted derivatives being most efficient (Table 1, entries 5–13,19–27,32–40). Nearly quantitative conversion of ca. 98–120 equivalents of *rac*-BPL^{CH_2ZPh} by **1d–1g** was reached within 6–15 min (Table 1, entries 7,12,21,26,35,38). The overall slightly faster rate of polymerization observed for BPL^{CH_2OPh} as compared to BPL^{CH_2SPh} (Tables 1,S1; Figure 1), regardless of the catalytic system, most likely arose from the relative instability of BPL^{CH_2SPh} at 20 °C, the secondary products formed (products **2** and **3**; Figure S9) presumably impeding the efficiency of the catalyst, hence altering the polymerization rate. Furthermore, the highest TOF values obtained for the ROP of $BPL^{CH_2OPh/CH_2SPh/CH_2CH_2OCH_2Ph}$ promoted by the catalytic systems **1d–1g**/(*i*PrOH) (450 < TOF (h^{-1}) < 1840; Table 1, entries 7,9,12,21,26,34–39) were significantly higher than those reported for the closely related alkoxymethylene β-propiolactones BPL^{CH_2OR}s (R = Me, Bn, All) similarly polymerized by these same yttrium catalytic systems (TOF = 54–100 h^{-1}),[8b,16] yet lower than those obtained from BPL^{CO_2R} monomers with pendant ester side-chains (R = Bn, All; TOF > 3000 h^{-1}).[15b] The overall trend for the monomers' ROP ability is thus BPL^{CH_2OPh} ≈ BPL^{CH_2SPh} > $BPL^{CH_2CH_2OCH_2Ph}$, while the catalysts' activity thus generally followed the order **1d–1g** >> **1a** ≈ **1b** >> **1c**, as previously reported for the previous ROP of various BPL^{FG}s β-lactones (FG = Me, CH$_2$OR, CO$_2$R) promoted by these catalyst systems.[7,15,16]

Monitoring of NMR-scale polymerizations of $BPL^{CH_2OPh/CH_2SPh/CH_2CH_2OCH_2Ph}$ performed with **1a–1g**/(*i*PrOH) confirmed the kinetics trend derived from batch experiments, and linear semi-logarithmic plots established that all reactions were first order in monomer (apparent rate constant k_{app} = 67.3 ± 3.1 min^{-1}, $BPL^{CH_2CH_2OCH_2Ph}$/**1d**; 32.93 ± 0.01 min^{-1}, BPL^{CH_2OPh/CH_2SPh}/**1d,1f**; 15.05 ± 0.38 min^{-1}, $BPL^{CH_2CH_2OCH_2Ph}$/**1f**; 0.76 ± 0.07 min^{-1}, BPL^{CH_2OPh}/**1a**; 0.58 ± 0.11 min^{-1}, BPL^{CH_2SPh}/**1a**; 9.05 ± 0.06 × 10^{-2} min^{-1}, BPL^{CH_2OPh}/**1c**; 6.69 ± 0.62 × 10^{-2} min^{-1}, $BPL^{CH_2CH_2OCH_2Ph}$/**1a**;

16

$4.25 \pm 0.43 \times 10^{-2}$ min^{-1}, BPL^{CH_2CH_2OCH_2Ph}/**1c**; $1.2 \pm 0.1 \times 10^{-2}$ min^{-1}, BPL^{CH_2SPh}/**1c** (Tables 1,S1, Figure 1).
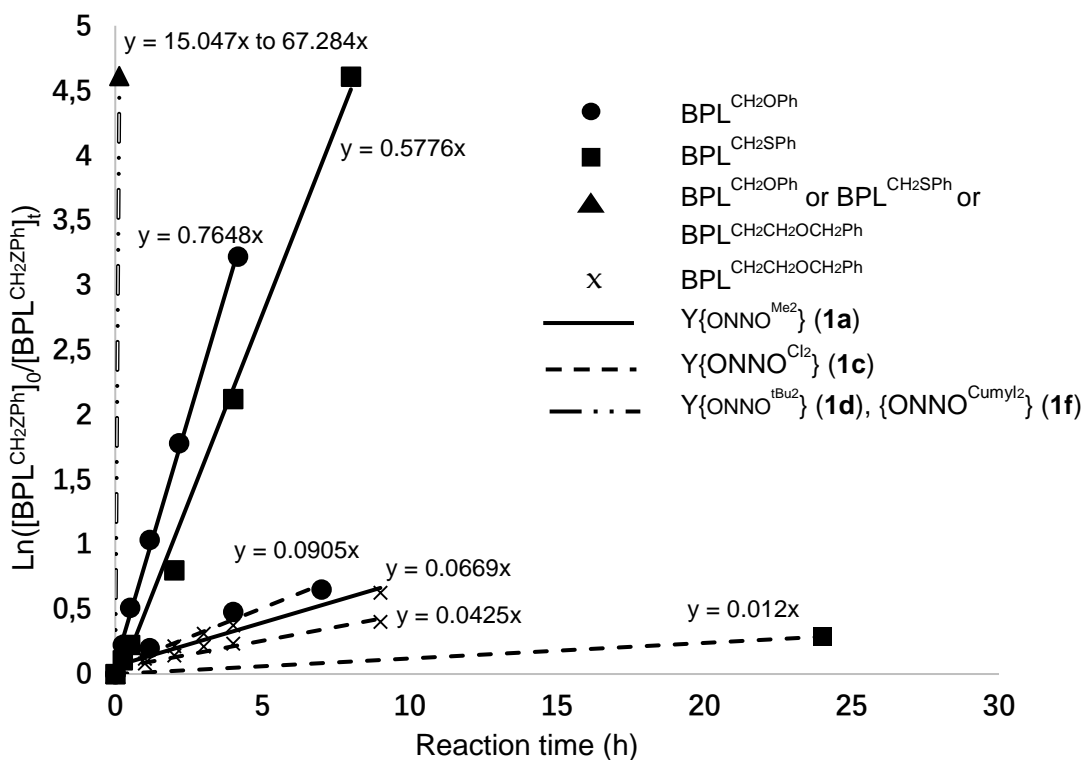
Figure 1. Semi-logarithmic first-order plots for the ROP of *rac*-BPL^{FG}s mediated by **1a,1c,1d,1f**/(*i*PrOH) (20 °C, toluene; [BPL^{CH_2ZPh}]$_0$/{[**1**]$_0$/[*i*PrOH]$_0$} = 60:1:1): **1a** (Table 1, entries 2,15; Table S1, entry 1); **1c** (Table 1, entries 4,18; Table S1, entry 2); plots for the ROPs mediated by **1d** (Table 1, entries 6,20; Table S1, entry 3) and **1f** (Table 1, entries 11,25; Table S1, entry 4), all overlap due to similar high activity of these catalysts regardless of the monomer, and are represented as ▲ .

All the PBPL^{CH_2ZPh}s isolated showed, regardless of the catalytic system used, a quite good agreement between the theoretical molar mass values ($M_{n,theo}$) and the experimental values determined by NMR ($M_{n,NMR}$) and by SEC ($M_{n,SEC}$) analyses. The latter experimental molar mass values of the PBPL^{CH_2ZPh}s increased linearly with the BPL^{CH_2ZPh} monomer loading up to a degree of polymerization of ca. 450, as illustrated for the ROP of BPL^{CH_2ZPh} mediated by the **1d** or **1g**/(*i*PrOH) (1:1) catalytic system (Figure 2; Table S1). The dispersities of all PBPL^{CH_2ZPh}s remained generally narrow

17

($Đ_M$ = 1.05–1.23), supporting a relatively fast initiation (compared to propagation) along with some limited undesirable side reactions (classically inter- and intra-molecular transesterification reactions (i.e. reshuffling and backbiting, respectively), or other transfer or termination reactions). Such dispersity values fell within the range of those typically obtained for the related *racemic* 4-substituted-β-propiolactones BPL[FG]s.[8,15,16] All these characteristics highlighted the controlled feature and to some extent the livingness of the ROP of the BPL[CH2ZPh]s mediated by **1a–1g**/(*i*PrOH) catalytic systems.
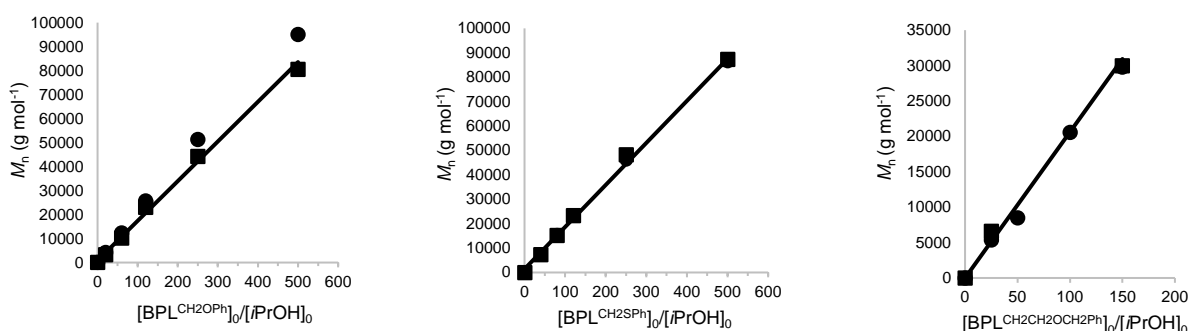
**Figure 2.** Variation of $M_{n,NMR}$ ■, $M_{n,SEC}$ ●, and $M_{n,theo}$ (solid line) values of PBPL[CH2ZPh]s synthesized from the ROP of *rac*-BPL[CH2ZPh]s mediated by **1d or 1g**/(*i*PrOH) (1:1) catalytic system as a function of the BPL[CH2ZPh] monomer loading (Table 1, entries 5–9;19–23;36–39).

**Macromolecular characterizations of PBPL[CH2ZPh]s synthesized by ROP of *rac*-BPL[CH2ZPh]s (Z = O, S, CH2OCH2) promoted by 1a–1g/(*i*PrOH) catalyst systems**

The PBPL[CH2ZPh]s were unambiguously characterized by 1D and 2D NMR spectroscopy and mass spectrometry (Tables 1,S1; Figures 3–5,S12–S18). All ^{1}H and ^{13}C{^{1}H}and J-MOD NMR spectra clearly displayed the characteristic signals corresponding to both the BPL[CH2ZPh] repeating units, especially the backbone methine and methylene signals, and the typical pendant CH2ZPh moieties, respectively (refer to the Experimental Section). The distinctive isopropoxycarbonyl chain-end group resonances were also clearly observed (δ (ppm): ca. 4.95 (CH₃)₂C*HO*–, ca. 1.19 (C*H₃*)₂CHO–), supporting the propagation from the Y{ONXO[R2]}/(*i*PrOH) active species (Figures 3–5,S12–S18).

18

Further support of the macromolecular structure of the PBPL^{CH_2ZPh}s was gained from ESI or MALDI-ToF mass spectrometry analyses (Figures S19–S21). The spectra recorded for low molar mass samples of PBPL^{CH_2ZPh}s prepared from **1d**,**1f**/*i*PrOH catalytic systems, showed a single population of macromolecules having a repeating unit of *m/z* 178, 194, or 206 ($M_{BPL(CH_2OPh)}$, $M_{BPL(CH_2SPh)}$, $M_{BPL(CH_2CH_2OCH_2Ph)}$), respectively, corresponding to α-isopropoxy,ω-hydroxyl telechelic PBPL^{CH_2ZPh} chains ionized by Na$^+$. This was unequivocally confirmed by the close match with the corresponding isotopic simulations, as illustrated for $[(CH_3)_2CHO(COCH_2CH(CH_2OC_6H_5)O)_nH]\cdot Na^+$ with, for example, calculated *m/z* 1507.551 versus found *m/z* 1507.548 for *n* = 8 (PBPL^{CH_2OPh}), for $[(CH_3)_2CHO(COCH_2CH(CH_2SC_6H_5)O)_nH]\cdot Na^+$ with, for example, calculated *m/z* 1053.2475 versus found *m/z* 1053.2473 for *n* = 5 (PBPL^{CH_2SPh}), and for $[(CH_3)_2CHO(COCH_2CH(CH_2CH_2OCH_2C_6H_5)O)_nH]\cdot Na^+$ with, for example, calculated *m/z* 3174.493 versus found *m/z* 3174.461 for *n* = 15 (PBPL^{CH_2CH_2OCH_2Ph}). Note that the second population observed in the MALDI-ToF mass spectrum of PBPL^{CH_2CH_2OCH_2Ph} corresponds to α-isopropoxy,ω-dehydrated (i.e., ω-crotonate) telechelic PBPL^{CH_2CH_2OCH_2Ph} chains ionized by Na$^+$, as unambiguously confirmed by the close match with the corresponding isotopic simulation for $[(CH_3)_2CHO(COCH_2CH(CH_2CH_2OCH_2C_6H_5)O)_nH-H_2O]\cdot Na^+$ with, for example, calculated *m/z* 3156.476 versus found *m/z* 3156.451 for *n* = 15. However, such a crotonate group was not detected in the NMR spectra of the prepared PBPL^{CH_2CH_2OCH_2Ph}s (no signals observed at δ$_{1H}$ 6.25, 5.77 ppm (C*H*=C*H*CH$_2$CH$_2$OCH$_2$Ph)), thus suggesting that the dehydration of the macromolecular chains occurred during the MALDI-ToF MS analysis or that it is a very minor population.
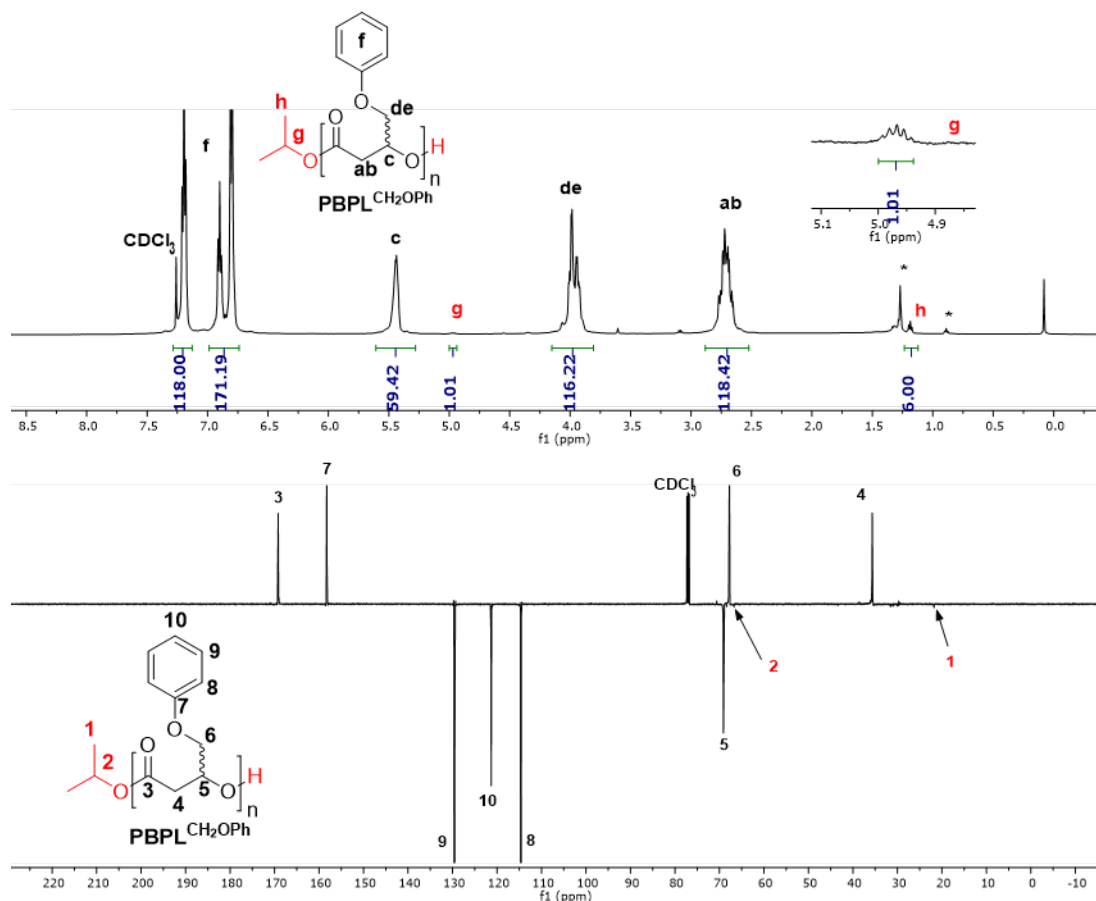
Figure 3. ^{1}H NMR (500 MHz, CDCl$_3$, 25 °C) (top) and J-MOD (125 MHz, CDCl$_3$, 25 °C) (bottom) spectra of syndiotactic PBPL^{CH_2OPh} prepared from the ROP of *rac*-BPL^{CH_2OPh} mediated by complex **1d** in the presence of *i*PrOH and precipitated twice in cold pentane (Table 1, entry 6) (*: residual grease).
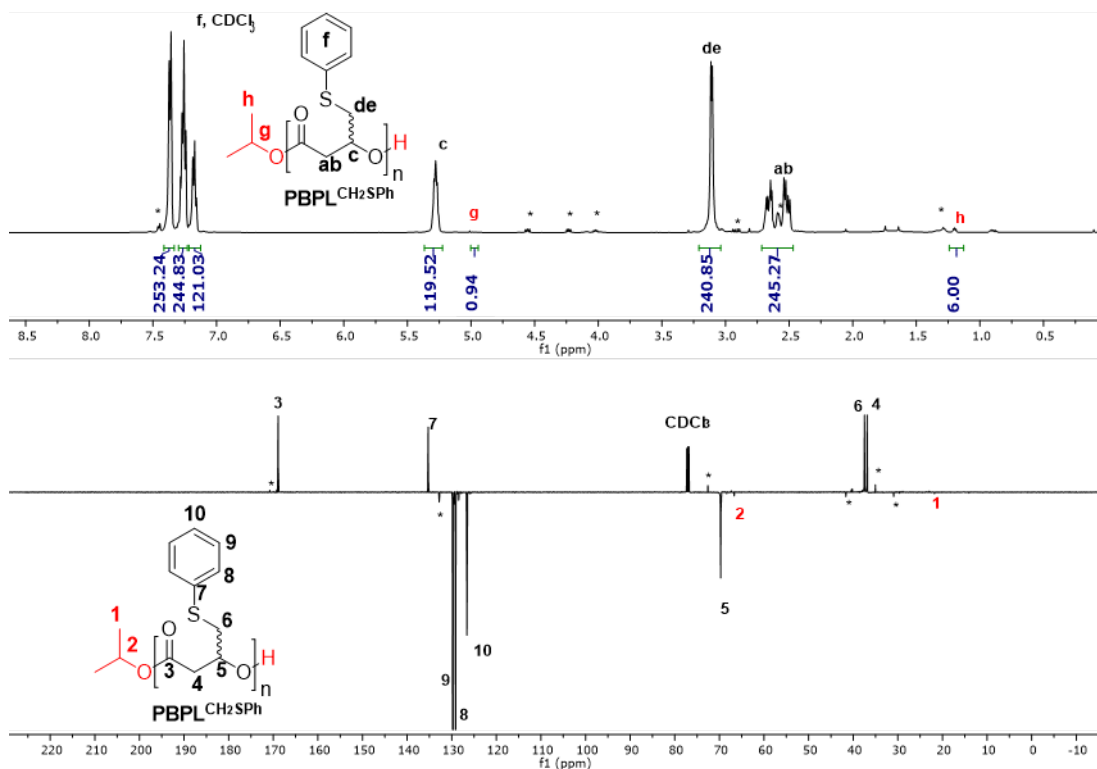
Figure 4. ^{1}H NMR (500 MHz, CDCl$_3$, 25 °C) (top) and J-MOD (125 MHz, CDCl$_3$, 25 °C) (bottom) spectra of syndiotactic PBPL^{CH_2SPh} prepared from the ROP of *rac*-BPL^{CH_2SPh} mediated by complex **1f** in the presence of *i*PrOH and precipitated twice in cold pentane (Table 1, entry 26) (*: minor peaks correspond to the degradation product **3** of BPL^{CH_2SPh}).
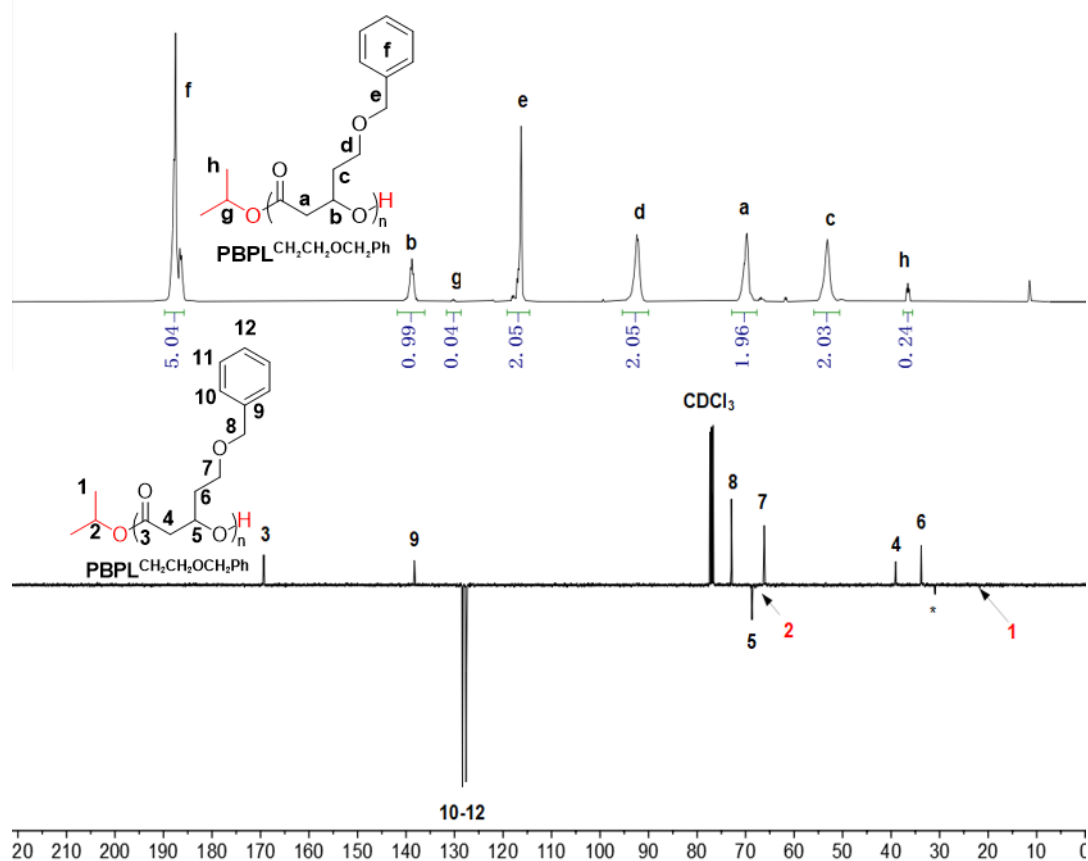
Figure 5. ^{1}H NMR (500 MHz, CDCl$_3$, 25 °C) (top) and J-MOD (100 MHz, CDCl$_3$, 25 °C) (bottom) spectra of syndiotactic PBPL^{CH_2CH_2OCH_2Ph} prepared from the ROP of *rac*-BPL^{CH_2CH_2OCH_2Ph} mediated by complex **1b** in the presence of *i*PrOH and precipitated twice in cold pentane (Table 1, entry 29).

Microstructural characterization of PBPL^{CH_2ZPh}s: Stereoselectivity of the catalysts 1a−1g/(*i*PrOH) in the ROP of *rac*-BPL^{CH_2ZPh}s (Z = O, S, CH$_2$OCH$_2$)

Motivated by the outstanding stereoselectivity of the achiral Y{ONXO^{R_2}}/(*i*PrOH) catalyst systems **1a−1g**/(*i*PrOH) in the ROP of chiral β-lactones,[8a,8b,15,16] the stereoregularity of the herein synthesized PBPL^{CH_2ZPh}s was closely examined. Most commonly, the stereocontrol in the ROP of chiral cyclic esters mediated by achiral metal catalyst systems originates from a so-called chain-end stereocontrolled mechanism (CEM) in which the chirality of each next incoming monomer unit is tuned by the chirality of the last monomer unit inserted into the growing polymer chain.[8] Thus, syndiotactic polymers are most often formed from CEM, since the active species

alternatively selects from a *racemic* monomer, the enantiomer with the opposite configuration in order to minimize the steric bulkiness in the transition state.

The tacticity of the recovered PBPL^{CH_2ZPh}s was thus assessed from ^{13}C NMR spectra analyses (upon comparison with the corresponding spectra of the isotactic PBPL^{CH_2ZPh}s synthesized from the enantiopure monomers, respectively (Figures S12−14,S18)) in close relationship with the nature of the exocyclic side-chain and the nature of the substituted phenolate ligand framework of the yttrium complexes **1a−1g**/(*i*PrOH) (Figure 6, Table 1). It is worth pointing out that the *rac*-BPL^{CH_2ZPh}s (Z = O, S, CH$_2$OCH$_2$) herein investigated ''simply'' differ from the previously studied *rac*-BPL^{CH_2OCH_2Ph} by one less methylene group in the phenoxide/phenylthiol moiety in the case of BPL^{CH_2OPh} and BPL^{CH_2SPh}, or by the replacement in the exocyclic pendant group of a methylene by an ethylene moiety in the case of BPL^{CH_2CH_2OCH_2Ph}. The stereoselectivity of the yttrium catalysts incorporating variously *ortho*-substituted phenolate ligands revealed different from one class of BPL^{FG} monomer to another; the stereoselectivity was strongly affected by the nature of the R *ortho*-substituents installed on the phenolate ligands and by the nature of the exocyclic functional group FG of the β-lactone monomer (Tables S2,S3).

First, no significant difference in terms of stereoselectivity of PBPL^{CH_2ZPh}s was observed to arise from the X donor group in the ''capping'' moiety of the {ONXO^{R_2}}$^{2-}$ ligand, similarly to the previous alike ROP of BPL^{FG}s with FG = Me, CH$_2$OR, C(O)OR.[8] Regardless of the catalyst system implemented, exchanging oxygen with sulphur in FG = CH$_2$ZPh (Z = O, S, i.e. BPL^{CH_2OPh} vs BPL^{CH_2SPh}) did not affect the stereochemistry of the resulting syndiotactic PBPL^{CH_2ZPh}s. This was different with PBPL^{CH_2CH_2OCH_2Ph} which revealed either syndiotactic or atactic, depending on the yttrium complex used, namely **1d−1g** or **1a−1c**, respectively. Generally, ^{13}C NMR spectra of the PBPL^{CH_2ZPh}s indicated that when the yttrium complex incorporated bulky substituents at the *ortho*-positions of the phenolate rings (*t*Bu or cumyl groups, **1d−1g**), syndio-enriched PBPL^{CH_2ZPh}s (P_r up to 0.77–0.87) were produced from *rac*-BPL^{CH_2ZPh}s, (Table 1, entries 5−12,19−26,32−39). In comparison, similarly highly syndiotactic PBPL^{CH_2OCH_2Ph}s were reported from *rac*-BPL^{CH_2OCH_2Ph} (P_r = 0.88–0.90).[16a]

23

ACCEPTED MANUSCRIPT

Unexpectedly and most strikingly, the use of an *ortho*-dichloro-substituted ligand in **1c** gave syndio-enriched PBPL$^{CH_2OPh/CH_2SPh}$ (P_r = 0.73–077) (Table 1, entries 3,4,17,18) and atactic PBPL^{CH_2CH_2OCH_2Ph} (P_r = 0.49) (Table 1, entry 31), in comparison to isotactic PBPL^{CH_2OCH_2Ph} (P_r = 0.10).[16a] Also, while the similarly uncrowded *ortho*-dimethyl-substituted ligand in **1a−1b** returned, similarly to the dichloro analogue **1c**, syndio-enriched PBPL$^{CH_2OPh/CH_2SPh}$ (P_r = 0.74–079) (Table 1, entries 1,2,14,15) and atactic PBPL^{CH_2CH_2OCH_2Ph} (P_r = 0.49–052) (Table 1, entry 28–30), it afforded atactic PBPL^{CH_2OCH_2Ph} (P_r = 0.50)[16a] and atactic PBPL^{Me} (P_r = 0.56).[12] Methylene groups apart from the exocyclic oxygen of the side-arm or a simple methyl substituent thus appeared detrimental to the stereoselectivity control promoted by uncrowded **1a−1c** catalysts.

The stereochemistry of the PBPL^{CH_2ZPh}s reported herein can be more largely compared to that of all the previously reported PBPL^{FG}s (FG = Me, CH$_2$OR, CO$_2$R with R = Me, All, Bn) similarly prepared by ROP of BPL^{FG} promoted by **1a−1g**/(*i*PrOH), as summarized in Tables S2,S3.[15,16] Considering the catalyst system based on **1c** flanked with an halogenated non-crowded ancillary ligand, the presence of two "CH$_2$" moieties apart from the central oxygen of the pendant FG = *CH$_2$OR* (R = Me (*CH$_3$*), All (*CH$_2$*CH=CH$_2$), Bn (*CH$_2$*Ph)), i.e. "*CH$_2$OCH$_2$*" in 4-alkoxymethylene-β-propiolactones BPL^{CH_2OR}s, was evidenced to be essential to afford highly isotactic PBPL$^{CH_2OMe/All/Bn}$s that arose from the presence of strong Cl…C–H non-covalent interactions (NCIs) between the chloro substituents and the two methylene groups.[16] The stereocontrol was then switched to syndiotacticity, either upon replacement of one of these methylenes into FG = C(O)OR of the β-malolactonates, or upon its removal into FG = C*H$_2$*OPh or C*H$_2$*SPh of the BPL^{CH_2ZPh}s (Z = O, S). Moreover, increasing the length of the pendant chain from alkoxymethylene "C*H$_2$*OCH$_2$" in BPL^{CH_2OR}s to alkoxyethylene "C*H$_2$*C*H$_2$*OCH$_2$" in BPL^{CH_2CH_2OCH_2Ph} seem to affect the Cl…C*H$_2$*s interactions. We assume this is possibly due to a different conformation in the monomer/active species interactions, and/or due to the decrease in acidity of the methine-adjacent methylenes of the side-chain in −C*H$_2$*C*H$_2$*OCH$_2$Ph vs −C*H$_2$*OCH$_2$Ph, ultimately weakening the NCIs and leading to the loss of stereocontrol to afford atactic polymers, similarly to those obtained with BPL^{Me}.[12b,c]

24

ACCEPTED MANUSCRIPT

The ROP of the β-lactones promoted by non-crowded non-halogenated yttrium catalysts, typically Me-substituted phenolate catalysts **1a–1b**, provided atactic PBPL[FG]s, except with BPL[CH2OPh/CH2SPh] and the β-malolactonate monomers[15] which returned syndio-enriched-to-highly syndiotactic polymers, respectively. This latter stereocontrol might then originate from the coordination to the yttrium center of the heteroatom (O, S) atom of the phenoxide (CH$_2$OPh), thiophenoxide (CH$_2$SPh) or alkoxycarbonyl (C(O)OR) of the side-group of the last inserted monomer unit of the growing chain, thereby forming a highly coordinated – and thus bulkier and more prone to stereoselectivity – rare earth active species.

Finally, when implementing crowded substituted phenolate ligands, *i.e* CMe$_2$Ph and *t*Bu, onto the yttrium active center **1d–1g**/(*i*PrOH), syndiotactic polymers were commonly produced regardless of the BPL[FG] exocyclic substituent (FG = Me, CH$_2$OPh, CH$_2$SPh or CH$_2$CH$_2$OCH$_2$Ph, CO$_2$All/Bn, CH$_2$OMe/All/Bn), in line with a CEM mechanism being at play. The results we report herein thus further highlight the strong dependence of the resulting PHA's stereocontrolled microstructure on the couple formed by the functional β-lactone and the yttrium catalyst, and more specifically on the chemical nature of the β-lactone side-arm and of the substituents on the metal surrounding ancillary.
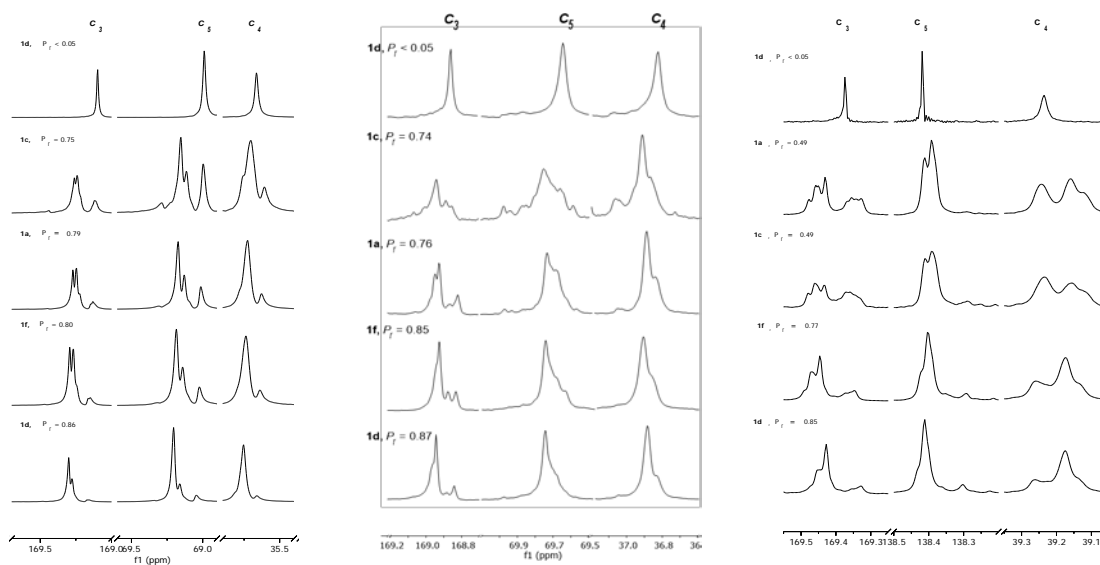
Figure 6. Regions of the ^{13}C{^{1}H} NMR spectra (125 MHz, CDCl$_3$, 23 ˚C) of PBPL[CH2ZPh]s prepared by ROP of *rac*-BPL[CH2ZPh]s (Z = O, S, CH$_2$OCH$_2$), except for the

top spectra: of enantiopure (S or R)-BPL^{CH_2ZPh}) (Table 1, entries 13,27,40), mediated by **1a**, **1c**, **1d**, or **1f** /(iPrOH): (left) PBPL^{CH_2OPh} (Table 1, entries 2,4,6,9), (middle) PBPL^{CH_2SPh} (Table 1, entries 15,18,20,25), (right) PBPL^{CH_2CH_2OCH_2Ph} (Table 1, entries 28,31,32,34).

Thermal characteristics of PBPL^{CH_2ZPh}s synthesized by ROP of *rac*-BPL^{CH_2ZPh}s (Z = O, S, CH$_2$OCH$_2$) promoted by 1a–g catalyst systems

The thermal behavior of the synthesized PBPL^{CH_2ZPh}s was analyzed by thermal gravimetry analysis (TGA) and differential scanning calorimetry (DSC) (Figures S22–S25). The PBPL^{CH_2OPh} and PBPL^{CH_2SPh} samples were found to thermally degrade at the same temperature ($T_d^{onset}{}_{PBPLCH2OPh}$ = 272 °C, $T_d^{onset}{}_{PBPLCH2SPh}$ = 271 °C) that is significantly higher than the one measured for PBPL^{Me} (T_d^{onset} = 256 °C) and PBPL^{CH_2CH_2OCH_2Ph} ($T_d^{onset}{}_{PBPLCH2CH2OCH2Ph}$ = 226 °C) (Figure S22). DSC thermograms only showed the presence of a glass transition temperature (T_g); no melting temperature was observed below 200 °C, suggesting amorphous polyesters (Tables 1,S2,S3; Figures S23–S25). This lack of crystallinity was similarly reported for the closely related syndiotactic or isotactic PBPL^{CH_2OCH_2Ph}, while a melting temperature was only observed for the syndiotactic PBPL$^{CH_2OMe/All}$ (T_m = 116, 85 °C) and PBPL$^{CO_2All/Bn}$ (T_m = 51–117 °C).[15b,16a] The T_g values were similarly observed to be closely related to the nature of the functional side-chain of the PHAs. The PBPL$^{CH_2OPh/CH_2SPh}$ displayed positive T_g values going from 8 to 14 °C for the phenoxymethylene substituent, up to 21 to 40 °C for the corresponding thiophenoxymethylene. On the other hand, the PBPL^{CH_2CH_2OCH_2Ph} polyester with the longer benzyloxyethylene pendant moieties, that most likely impart more mobility to the macromolecular chains, showed the lowest T_g (typically T_g = −12 °C) − and T_d as well − values.

The influence of the stereoenrichment of PBPL^{CH_2ZPh}s on T_g showed, as anticipated, higher T_g values for the most syndiotactic polymers as compared to the less syndio-enriched ones (Tables 1, S1; Figures S23–S25). Typically, for PBPL^{CH_2OPh}s with P_r = 0.75–0.79, the T_g values varied from 21 to 30 °C, while a higher syndio-enrichment with P_r = 0.83–0.87 or an almost purely isotactic sample (P_r < 0.05) resulted in higher

T_g values ranging from 36 to 40 °C. The same trend was observed with PBPL^{CH_2SPh}s that displayed T_g values varying from 8–9 °C for samples with $P_r = 0.73$–0.76, while more syndio-enriched polymer samples with $P_r = 0.83$–0.87 or an almost purely isotactic sample ($P_r < 0.05$) gave higher T_g values ranging from 12 to 14 °C. The trend is, as expected, similar to the previously reported thermal behavior of the related PBPL^{CH_2OCH_2Ph} that showed a T_g value going from −6 °C to −2 and to 0 °C upon improving the stereoregularity of the polyesters from atactic (P_r ca. 0.50) to syndiotactic (P_r ca. 0.85 −0.90) and isotactic (P_r ca. 0.10), respectively.[16] No distinct tendency in the T_g values of PBPL^{CH_2CH_2OCH_2Ph} samples was however observed.

Conclusion

The unprecedented functional PBPL^{CH_2ZPh}s with Z = O, S, CH$_2$OCH$_2$ have been easily and successfully prepared from the controlled ROP of the corresponding *racemic* 4-substituted-β-propiolactones *rac*-BPL^{CH_2ZPh}s, mediated by diamino- or amino-alkoxy-bis(phenolate) yttrium amido complexes **1a–1g** in the presence of isopropanol as co-initiator. All yttrium complexes revealed active, affording well-defined high molar mass PHAs with a good control of the polymerization in terms of molar mass values and limited undesirable side reactions ($M_{n,NMR}$ up to 86,400 g mol^{-1}, $Đ_M < 1.23$).

The best activities reached by the yttrium complexes **1d–1g** with the most crowded substituents installed on the tetradentate bisphenolate ligand (e.g. *t*Bu, CMe$_2$Ph), in the ROP of these β-lactones (typically $225 < $ TOF (h^{-1}) ≤ 1840), revealed significantly higher than those achieved with the related *rac*-4-alkoxymethylene-β-propiolactones BPL$^{CH_2OMe/All/Bn}$ ($1 < $ TOF (h^{-1}) $<$ ca. 100),[16] yet lower than the record value established with the ROP of *rac*-β-malolactonates BPL^{CO_2R} (TOF ≥ 3000 h^{-1}).[15] On the other hand, catalysts with less-crowded phenolate substituents (e.g. Me, Cl) revealed significantly less active in the ROP of *rac*-BPL^{CH_2ZPh}s, with the chloro derivative **1c** being sluggish, as previously observed in the ROP of BPL$^{CH_2OAll/Bn}$.[8b]

Highly *syndiotactic* PBPL^{CH_2OPh} and PBPL^{CH_2SPh}s were always obtained (P_r up to 0.87), unrelatedly to the O or S heteroatom and regardless of the yttrium catalyst, and similarly to syndiotactic PBPL^{Me}, PBPL$^{CH_2OMe/All/Bn}$, and PBPL$^{CO_2All/Bn}$.[8,12,15,16] On the

27

other hand, the simple modification of *ortho*-R substituents on the $\{ONOO^{R_2}\}^{2-}$ ligand platform from uncrowded to crowded, allowed a complete reversal from a *nonselective* (P_r ca.0.50 with R = Cl, Me) to highly *syndioselective* (P_r up to 0.86 with R = cumyl, *ter*-butyl) ROP of $BPL^{CH_2CH_2OCH_2Ph}$, respectively. The intimate relationship between the chemical nature of the exocyclic functional side-group on the β-lactone and the stereoelectronic tuning arising from the phenolate ligand *ortho*-substituents on the yttrium coordination sphere, is evidenced in the control of the stereoselectivity of the ROP through the implementation – or not – of NCIs. These achiral rare earth catalyst systems thus afforded a remarkable stereocontrol in the ROP of original functional *racemic* β-lactones, among which the first sulphur-substituted PHAs, ultimately providing PHAs with tunable thermal properties, and further highlighting their valuable potential.

Conflicts of interest

There are no conflicts to declare.

References

1   (a) The Handbook of Polyhydroxyalkanoates (2021) CRC Press, Taylor & Francis Group, Boca Raton, Koller M. (ed.); (b) B. Laycock, P. Halley, S. Pratt, A. Werker and P. Lant, *Prog. Polym. Sci.* 2013, **38**, 536-583; (c) S. Taguchi, T. Iwata, H. Abe and Y. Doi (2012) Poly(hydroxyalkanoate)s, in Polym. Sci.: A Comprehensive Ref., Volume 9, K. Matyjaszewski and M. Möller (eds.); (d) G. Q. Chen, *Chem. Soc. Rev.* 2009, **38**, 2434-46; (e) J. Lu, R. C. Tappel and C. T. Nomura, *Polym. Rev.*, 2009, **49**, 226–248.

2   (a) European Bioplastics, nova Institute (2020); https://www.european-bioplastics.org/market/ and https://www.bio-based.eu/markets; (b) Global PHA market value 2019 & 2024, Published by Ian Tiseo, Jan 27, 2021, MarketsandMarkets © Statista 2021; https://www-statista-com; (c) Jan Ravenstijn, PHA's: the natural materials of the future, in GO!PHA White Paper - 26 July 2019.

3   (a) K. W. Meereboer, M. Misra and A. K. Mohanty, *Green Chem.*, 2020, **22**, 5519-5558; (b) M. Koller, L. Maršálek, M. M. de Sousa Dias and G. N. Braunegg, *Biotechnol*. 2017, **37**(Pt A), 24-38. (c) L. R. Lizarraga-Valderrama, B. Panchal, C. Thomas, A. R. Boccaccini and I. Roy, Biomedical Applications of Polyhydroxyalkanoates, in Biomaterials from Nature for Advanced Devices and Therapies, First Edition, Chapter 20 (2016), Nuno M. Neves and Rui L. Reis (eds.); (d) A. Anjum, M. Zuber, K. M. Zia, A. Noreen, M. N. Anjum and S. Tabasum, *Int. J. Biological Macromol.* 2016, **89**, 161–174; (e) S. F. Williams and D. P. Martin, Applications of Polyhydroxyalkanoates (PHA) in Medicine and Pharmacy, Polyesters, in Biopolymers Online, Part 4. Chap 20, A. Steinbüchel (ed.) (2005); (f) R. W. Lenz and R. H. Marchessault, *Biomacromolecules*, 2005, **1**, 1-8; (g) R. A. Gross and B. Kalra, *Science* 2002, **297**, 803-807.

4   (a) M. Venkateswar Reddy, Y. Mawatari, R. Onodera, Y. Nakamura, Y. Yajima, Y.-Cheol Chang, *Bioresource Technology Reports* 2019, **7**, 100246; (b) Z. Li, J. Yang, X. J. Loh, *NPG Asia Mater*. 2016, **8**, e265; (c) A. Anjum, M. Zuber, K. M. Zia, A. Noreen, M. N. Anjum, S. Tabasum, *Int. J. Biol. Macromol.* 2016, **89**, 161–174; (d) M. Shabina, M. Afzal, S. Hameed, *Green Chem. Lett. Rev*. 2015, **8**, 56–77; (e) M. N. Somleva, O. P. Peoples, K. D. Snell, *Plant Biotechnol. J.* 2013, **11**, 233 –252.

5   (a) S. Taguchi, T. Iwata, H. Abe, Y. Doi in Polymer Science: A Comprehensive Reference (Ed.: M. Mçller), Elsevier, Amsterdam, 2012, pp. 157–182; (b) G.-Q. Chen in Plastics from bacteria: Natural functions and applications, Vol. 14 (Ed.: G.-Q. Chen), Springer, Berlin, 2010, pp. 17–37; (c) K. Sudesh, H. Abe, Y. Doi, *Prog. Polym. Sci.* 2000, **25**, 1503–1555; (d) Y. Poirier, C. Nawrath, C. Somerville, *Nat. Biotechnol.* 1995, **13**, 142.

6   D. J. Walsh, M. G. Hyatt, S. A. Miller and D. Guironnet, *ACS Catal.* 2019, **9**, 1115311188.

7   D. M. Lyubov, A. O. Tolpygin and A. A. Trifonov, *Coord. Chem. Rev.* 2019, **392**, 83-145.

8   (a) H. Li, R. M. Shakaroun, S. M. Guillaume and J.-F. Carpentier, *Chem. – Eur. J.*, 2020, **26**, 128-138; (b) R. Ligny, M. M. Hänninen, S. M. Guillaume and J.-F. Carpentier, *Chem. Commun.* 2018, **54**, 8024-8031; (c) S. M. Guillaume, E. Kirilov, Y. Sarazin and J.-F. Carpentier, *Chem. – Eur. J.*, 2015, **21**, 7988–8003; (d) J.-F. Carpentier, *Organometallics* 2015, **34**, 4175-4189; (e) N. Ajellal, J.-F.

Carpentier, C. Guillaume, S. M. Guillaume, M. Helou, V. Poirier, Y. Sarazin and A. Trifonov *J. Chem. Soc. Dalton Trans.* 2010*,* **39**, 8363-8376.

9   (a) C. Bakewell, A. J. White, N. J. Lon and C. K., Williams, *Angew. Chem. Int. Ed.* 2014, **53**, 9226-9230; (b) T.-Q. Xu, G.-W. Yang, C. Li and X.-B. Lu, *Macromolecules* 2017, **50**, 515-522.

10   (a) Z. Zhuo, C. Zhang, Y. Luo, Y. Wang, Y. Yao, D. Yuan and D. Cui, *Chem. Commun.* 2018, **54**, 11998-12001; (b) D. Pappalardo, M. Bruno, M. Lamberti and C. Pellecchia, *Macromol. Chem. Phys.* 2013, **214**, 1965-1972.

11   (a) J. Kiriratnikom, C. Robert, V. Guérineau, V. Venditto and C M. Thomas, *Frontiers in Chemistry* 2019, **7**, 301*;* (b) J. Fang, M. J. L. Tschan, T. Roisnel, X. Trivelli, R. M. Gauvin, C. M. Thomas and L. Maron, *Polym. Chem.* 2013, **4** , 360-367.

12   (a) Y. Chapurina, J. Klitzke, O. Casagrande, M. Awada, V. Dorcet, E. Kirillov and J. F., Carpentier, *Dalton Trans* 2014, **43**, 14322-14333; (b) M. Bouyahyi, N. Ajellal, E. Kirillov, C. M. Thomas and J.-F. Carpentier, *Chem. – Eur. J.*, 2011, **17**, 1872-1883; (c) A. Amgoune, C. M. Thomas, S. Ilinca, T. Roisnel and J.-F. Carpentier, *Angew. Chem. Int. Ed.* 2006, **45**, 2782 –2784; (d) A. Amgoune, C. M. Thomas, T. Roisnel and J.-F. Carpentier, *Chem. –Eur. J.*, 2006, **12**, 169 – 179; (e) C.-X. Cai, A. Amgoune, C. W. Lehmann and J.-F. Carpentier, *Chem. Commun.*, 2004, **3**, 330–331.

13   J.-B. Zhu and E. Y.-X. Chen, *Angew. Chem. Int. Ed.* 2019, **58**, 1178-1182.

14   W. Guerin, A. K. Diallo, E. Kirilov, M. Helou, M. Slawinski, J.-M. Brusson, J.-F. Carpentier and S. M. Guillaume, *Macromolecules* 2014, **47**, 4230−4235.

15   (a) C. G. Jaffredo, Y. Chapurina, E. Kirillov, J. F. Carpentier and S. M. Guillaume, *Chem. – Eur. J.*, 2016, **22**, 7629-7641; (b) C. G. Jaffredo, Y. Chapurina, E. Kirillov, S. M. Guillaume and J. F. Carpentier, *Angew Chem Int. Ed.* 2014, **53**, 2687-2691.

16   (a) R. Ligny, M. M. Hänninen, S. M. Guillaume and J.-F. Carpentier, *Angew. Chem. Int. Ed.* 2017, **56**, 10388-10393; (b) R. Ligny, S. M. Guillaume and J. F. Carpentier, *Chem. –Eur. J.*, 2019, **25**, 6412–6424.

17   J. W. Kramer, D. S. Treitler and G. W. Coates, *Org. Synth.* 2003, **86**, 287-297.

18   R. Anwander, O. Runte, J. Eppinger, G. Gerstberger, E. Herdtweck and M. Spiegler, *J. Chem. Soc., Dalton Trans.* 1998, 847-858.

19   T. D. Montgomery and A. B. Smith III, *Org. Lett.* 2017, **19**, 6216-6219.

20   H. Choi, S.-Y. Ham, E. Cha, Y. Shin, H.-S. Kim, J. K. Bang, S.-H. Son, H.-D. Park and Y. Byun, *J. Med. Chem.* 2017, **60**, 9821-9837.

21   S. E. Schaus, B. D. Brandes, J. F. Larrow, M. Tokunaga, K. B. Hansen, A. E. Gould, M. E. Furrow and E. N. Jacobsen, *J. Am. Chem. Soc.* 2002, **124**, 1307-1315.

22   (a) W. F. Edgell and J. Lyford IV, *Inorg. Chem.* 1970, **9**, 1932-1933; (b)

Wöltinger, J. E. Bäckvall and Á. Zsigmond, *Chem. Eur. J.* 1999, **5**, 1460-1467.

23   G. Adamus, I. Kwiecien, M. Maksymiak, T. Bałakier, J. Jurczak, and M. Kowalczuk, *Analytica Chimica Acta*, 2014, **808**, 104–114.